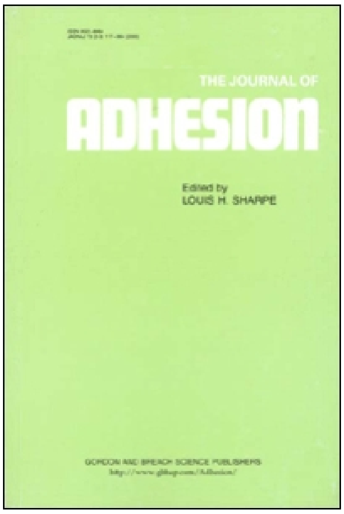

The Journal of Adhesion
Publication details, including instructions for authors and subscription information:
http://www.informaworld.com/smpp/title~content=t713453635

THE DEVELOPMENT OF A MANDREL PEEL TEST FOR THE MEASUREMENT OF ADHESIVE FRACTURE TOUGHNESS OF EPOXY-METAL LAMINATES

L. F. Kawashita[a]; D. R. Moore[a]; J. G. Williams[a]
[a] Mechanical Engineering Department, London, UK

Online publication date: 18 June 2010

To cite this Article Kawashita, L. F. , Moore, D. R. and Williams, J. G.(2004) 'THE DEVELOPMENT OF A MANDREL PEEL TEST FOR THE MEASUREMENT OF ADHESIVE FRACTURE TOUGHNESS OF EPOXY-METAL LAMINATES', The Journal of Adhesion, 80: 3, 147 — 167

To link to this Article: DOI: 10.1080/00218460490279215

URL: http://dx.doi.org/10.1080/00218460490279215

The Journal of Adhesion, 80: 147–167, 2004

ISSN: 0021-8464 print/1545-5823 online
DOI: 10.1080/00218460490279215

Taylor & Francis
Taylor & Francis Group

THE DEVELOPMENT OF A MANDREL PEEL TEST FOR THE MEASUREMENT OF ADHESIVE FRACTURE TOUGHNESS OF EPOXY–METAL LAMINATES

L. F. Kawashita
D. R. Moore
J. G. Williams
Mechanical Engineering Department,
Imperial College London,
London, UK

A mandrel peel test is established for measuring the adhesive fracture toughness of a metal/rubber-toughened epoxy laminate system. By adopting an energy balance analysis it is possible to determine directly both adhesive fracture toughness and plastic work in bending the peel arm around the mandrel. The suitability of the procedure is examined for various types of metal peel arms, which are classified in terms of their ability to deform plastically during the test. The plastic work is also predicted theoretically, and comparisons are made between the measured and calculated values. The fracture energies determined from the mandrel tests are compared with those obtained from 90° fixed-arm peel tests. For the calculations of plastic work in bending in the fixed arm test, various options are used when modelling the tensile stress-strain behaviour of the peel arm material. In addition, the adhesive layer thickness is considered in terms of its influence on the calculation of adhesive fracture toughness.

Keywords: Adhesive fracture toughness; Peel strength; Metal-polymer laminates; Fracture mechanics; Mandrel peel; Fixed arm peel; Plastic work

Received 14 July 2003; in final form 20 October 2003.

Presented in part at the 26th Annual Meeting of The Adhesion Society, Inc., held in Myrtle Beach, South Carolina, USA, 23–26 February, 2003.

The authors acknowledge support from an EPSRC Platform grant, Support for D. R. Moore from a Royal Academy of Engineering senior research fellowship, and collaboration from IMRE, Singapore, for L. F. Kawashita.

Address correspondence to D. R. Moore, Mechanical Engineering Department, Room 806, Imperial College, South Kensington Campus, London SW7 2AZ, UK. E-mail: r.moore@imperial.ac.uk

INTRODUCTION

Laminates of metallic substrates and polymeric adhesives are used in a wide range of applications, particularly in the aerospace, automotive, and electronic industries. A key requirement is for adequate adhesion that is measured in various forms of peel tests. In each of these standard procedures [1–4], peel strength is determined and used as the measurement of adhesive strength. However, peel strength is not exclusively the energy necessary to propagate a crack through the adhesive or interface, but it includes other energies like the plastic work in bending the peel arm. Therefore, the aim in this work is to develop an experimental procedure which accounts for the main energy losses and to compare these results with a theory developed previously for fixed-arm tests [5, 7].

Fixed-Arm Peel

The energy contributions to a fixed-arm peel procedure can be described by a global energy analysis [5]. The input energy to the peel test needs to be resolved into the various deformational energies—elastic, plastic, and adhesive fracture energies, at least:

$$G_A = \frac{dU_{ext}}{bda} - \frac{dU_s}{bda} - \frac{dU_{dt}}{bda} - \frac{dU_{db}}{bda}, \tag{1}$$

where G_A is the adhesive fracture toughness; U is energy; subscripts ext, s, dt, and db refer to external work, strain energy, dissipated tensile energy, and dissipated bending energy, respectively; b is the specimen width; and da the peel fracture length. This approach has been applied to a fixed-arm peel test [5] in order to convert peel strength (P/b) to adhesive fracture toughness:

$$G_A = G_E - G_P, \tag{2}$$

where G_E is the input energy after correction for elastic deformation in the peel arm and G_P is the plastic work in bending the peel arm. The elastic corrections are often negligible [6], and the input energy is given by

$$G_E = \frac{P}{b}(1 - \cos\theta), \tag{3}$$

where θ is the peel angle. In order to calculate the plastic deformation energy associated with the peel arm, it is first necessary to have knowledge of the tensile stress-strain characteristics of the peel arm material. This will include an initial elastic deformation but also a subsequent work hardening (or plastic) deformation. The peel test may be modelled as a beam on an elastic foundation, and the plastic work in bending can be derived using large displacement beam theory. Kinloch *et al*. [5, 7, 8] formulated the problem for bilinear and power law work-hardening peel arms. When $\varepsilon \leq \varepsilon_y$,

$$\sigma = E\varepsilon \tag{4}$$

for both cases, and when $\varepsilon > \varepsilon_y$,

$$\sigma = \sigma_y \left(\frac{\varepsilon}{\varepsilon_y}\right)^N \tag{5}$$

for the power law work-hardening model and

$$\sigma = \sigma_y + \alpha E(\varepsilon - \varepsilon_y) \tag{6}$$

for the bilinear model, where σ_y is yield stress and ε_y is yield strain.

For laminates where the adhesive layer thickness (h_a) is very small, $h_a \rightarrow 0$, there is no requirement to consider the deformation in the adhesive in conducting the calculations of adhesive fracture toughness [7]. However, when h_a is considerable, the deformation in the adhesive layer should be included in the analysis for which it will be necessary to have knowledge of the elastic modulus of the adhesive. In all, these various calculations can be complex, and while a theoretical analysis is given in Georgiou *et al*. [7], software that can be used to conduct the calculations is available on the Imperial College London website [9].

Mandrel Peel

An alternative approach to the determination of adhesive fracture toughness is a mandrel peel test [10, 11]. This method involves peeling around a circular mandrel while applying an alignment load to the base of the laminate in order to ease conformation of the peel arm to the mandrel. A particular advantage of the procedure lies in its direct experimental measurement of both G_A and G_P.

Figure 1 shows a schematic diagram of a mandrel peel test. The peel arm is bent around a roller, and the plastic work is constant and independent on the fracture toughness. Two specimens with the same peel arm are tested: (1) an unbonded specimen, from where plastic work and friction coefficients are measured; and (2) the bonded laminate.

Breslauer and Troczynski [11] gave an account of the energy balance during the tests. When the laminate is bonded, the relationship between peel force (P) and alignment force (D_1) is given by

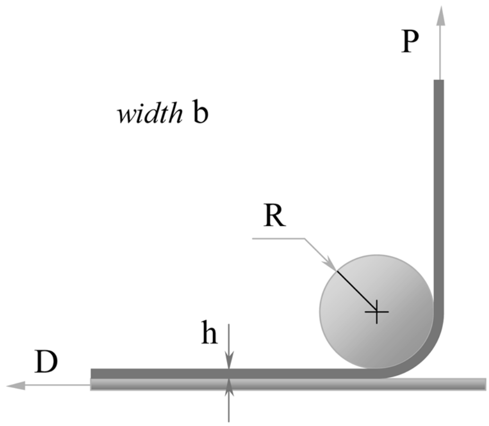

FIGURE 1 Configuration of a mandrel peel test.

$$P(1-\mu) = D_1 + b(G_A + G_P), \tag{7}$$

where μ is the coefficient of friction and G_P is the plastic work. For the unbonded specimen G_A is zero and the relationship becomes

$$P(1-\mu) = D_2 + bG_P, \tag{8}$$

where D_2 is the alignment force for the unbonded specimen. The terms G_A, μ, and G_P can then be obtained from plots of P/b *versus* D/b, as shown in Figure 2.

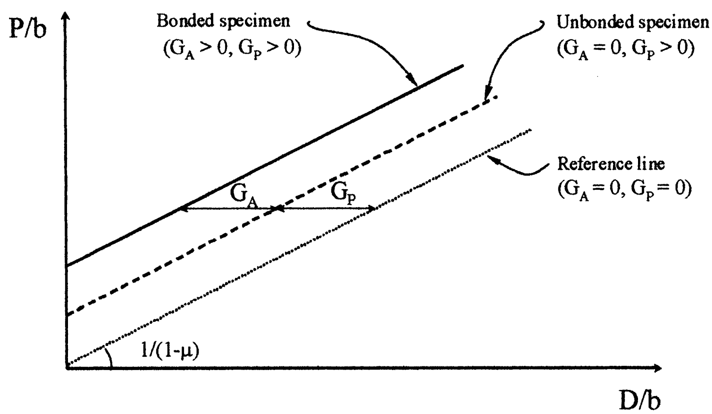

FIGURE 2 Schematic of data analysis for mandrel peel test.

The slope of both "bonded" and "unbonded" curves is proportional to the overall friction of the system. A reference line that intercepts the origin with the same slope is also shown in Figure 2. If the plastic work is zero (*e.g.*, by using a large radius mandrel), then the reference and the unbonded lines are the same, but this was not the case for the experiments presented in this work.

It is also possible to calculate G_P in a mandrel test by using the fixed-arm peel theory. The plastic energy term is given by [7]

$$G_P = \frac{E\varepsilon y^2 h}{2} f(k_0), \tag{9}$$

where k_0 is the maximum curvature of the adherendt, E is an elastic modulus of the peel arm material, h is its thickness, and ε_y is its yield strain. $f(k_0)$ is described fully in Georgiou *et al*. [7] and is dependent on the stress-strain model and loading–unloading conditions. The maximum curvature is given by [8]

$$k_0 = \frac{h}{2\varepsilon_y R_0}, \tag{10}$$

where R_0 is the minimum radius of curvature. In a mandrel test, R_0 is defined by the mandrel radius and the peel arm thickness, namely

$$R_0 = R + \frac{h}{2}, \tag{11}$$

which is independent of the fracture toughness.

EXPERIMENTAL

An apparatus for conducting mandrel peel tests was developed and is shown on the lefthand side of Figure 3. This apparatus included a linear bearing system onto which was mounted an aluminium plate that formed the base plate of the metal–polymer–metal laminate. The linear bearing system minimized the friction during the movement of the plate assembly during the test. The top substrate was the metal peel arm which was passed around the mandrel and connected to an Instron universal testing machine (Instron, High Wycombe, UK). The movement of the base plate on the linear bearing system was 100 mm, and an excess of 60 kg of alignment load could be attached to a pulley system that in turn was connected to the base plate. Mandrel rollers of radius ranging from 5 to 20 mm could be mounted in line with the peel arm. The mandrel rollers included bearings in order to minimise the frictional forces imposed by the peel arm.

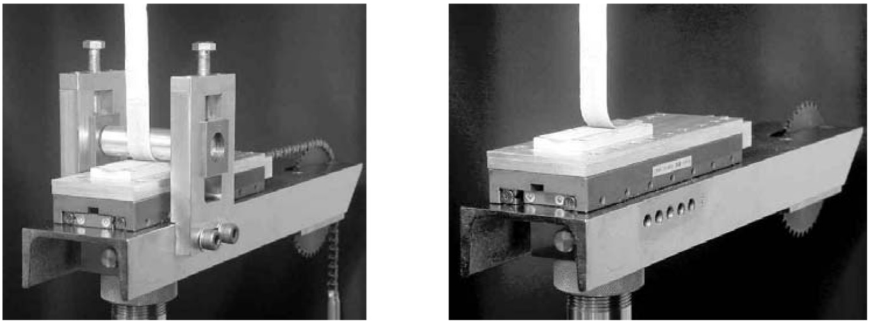

FIGURE 3 Mandrel jig apparatus in mandrel peel test configuration (left) and fixed-arm peel test configuration (right).

These were also quantified from the peel data as described by Equations (7) and (8), and the friction coefficients were typically under 3%.

The mounting brackets, which house the mandrel roller, could be removed from the apparatus in order to convert the jig into a 90° fixed-arm peel apparatus. This is shown in the right hand photograph in Figure 3. The linear bearing system remained on the apparatus so that peel proceeded with minimal frictional forces.

Preparation of the laminate was also a critical step in obtaining reliable data from the mandrel jig. A rubber-toughened (RT) single-part epoxy adhesive for general structural applications, Permabond ESP110, (Permabond Southampton, UK; tensile modulus 4.0 GPa, Poisson's ratio 0.4, and tensile yield stress 50 MPa) [12] was adhered between the aluminium base plate and the metallic foil. A special jig was constructed in order to house the laminates during preparation and cure (45 min at 150°C). In the mandrel peel tests, the peel arms were aluminium alloy (AA) ISO 5457-O and low-carbon (LC) steel, both with a nominal thickness of 1 mm. For further investigations on the validity of the mandrel test, additional foils were used, namely aluminium and copper, at a nominal thickness of 152 μm.

Specimen dimensions for all the laminates were as follows:

- Base plate (aluminium): width 30 mm, length 75 mm, thickness 4 mm
- Peel arm (various metals): width 16 mm, length 200 mm, thickness variable
- Bond-line: width 16 mm, length 75 mm, thickness about 400 μm.

All metallic substrates were grit blasted and later degreased in carbon tetrachloride. The aluminium surfaces were etched in a chromic acid solution. The aim was to provide bonded laminates where the peel fracture was cohesive in the adhesive.

In order to calculate the elastic and plastic deformation energies associated with the peel arm, it was first necessary to have knowledge of the tensile stress-strain characteristics of the peel arm material. Tensile tests on the peel arm materials were conducted on an Instron universal testing machine. Although there is little new in the determination of these properties, there was a special need to give attention to the accuracy in the measurement of tensile strain, particularly at small values. A video extensometer was used in all tests.

RESULTS AND DISCUSSION

Tensile Tests

A tensile stress-strain measurement on the peel arm provides data for elastic and plastic deformations and also a value of yield strain, as shown in Figure 4. This enables the calculation of plastic work that is then used to determine adhesive fracture toughness. The tensile stress-strain curve must be modelled by a bilinear function (as shown in Figure 5) or a power law (as shown in Figure 6) to enable the calculation of the plastic work by the theory presented in Georgiou *et al.* [7]. However, by examination of Figures 5 and 6, it is apparent that neither of these options provides a perfect fit for either 1 mm Al alloy or 1 mm steel peel. A third option has also been used, as shown in Figure 7, for a bilinear fit up to 5% strain. The three models were used in order to analyse their influence on the final results. The models

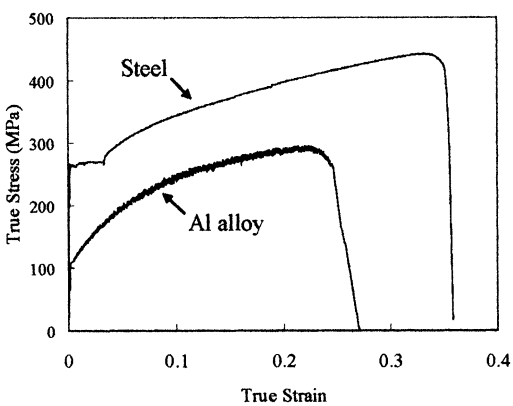

FIGURE 4 Tensile stress-strain curves for 1 mm AA and 1 mm steel peel arms.

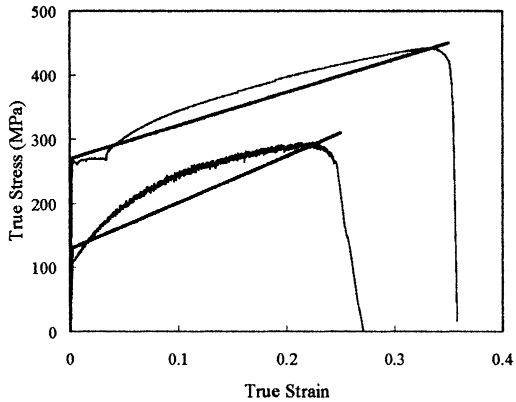

FIGURE 5 Tensile stress-strain curves from Figure 4 with full bilinear function fits.

were applied according to the requirements of Equations (4) to (6) and were as follows:

1. *A power law hardening function.*
2. A bilinear function that averages the full plastic work. This is designated *full bilinear function.*
3. A bilinear function that fits a plastic modulus to the plastic deformational data up to a strain of 5%. This is designated *5% strain bilinear function.*

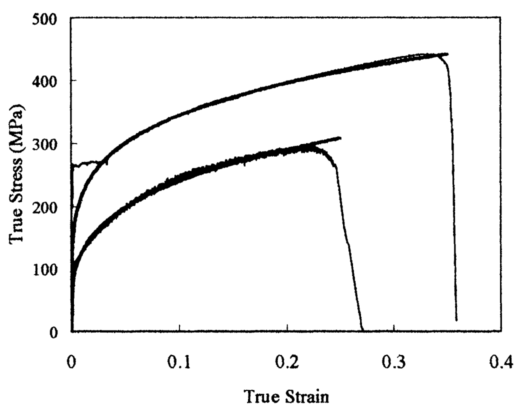

FIGURE 6 Tensile stress-strain curves from Figure 4 with power law fits.

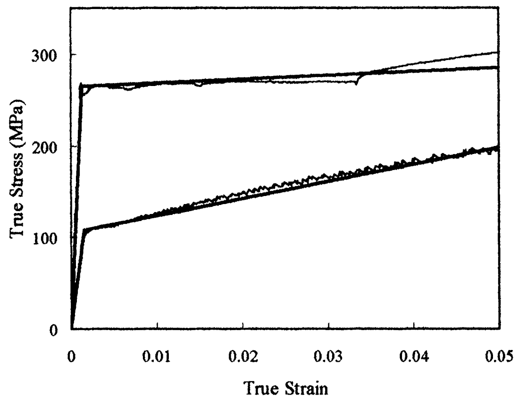

FIGURE 7 Tensile stress-strain curves from Figure 4 with 5% strain bilinear function fits.

The material parameters obtained from these models are shown in Tables 1 and 2.

Mandrel Peel Test Results

The mandrel peel tests are divided in to two parts: (1) a test with an unbonded specimen (adhered to the lower plate at one end only) and (2) a test on a fully bonded specimen. The peel arm is passed around the mandrel and attached to the universal testing machine. For both tests, the relationship between peel force per unit width (P/b) and alignment force per unit width (D/b) is investigated.

An example of calibration data (unbonded laminate) for 1 mm AA peel arm is shown in Figure 8. These results are typical of the consistency associated with these data, fitting well to a straight line (the coefficient of correlation, R^2, is 0.999967 for these data). When there

TABLE 1 Mechanical Properties of Al Alloy Peel Arms Based on Three Models

	Power-law hardening function	Full bilinear function	5% strain bilinear function
Elastic modulus E (GPa)	69	69	69
Yield strain e_y (%)	0.100	0.197	0.156
Power-law N	0.275	—	—
Bilinear coeff. α	—	0.011	0.027

TABLE 2 Mechanical Properties of Steel Peel Arms Based on Three Models

	Power-law hardening function	Full bilinear function	5% strain bilinear function
Elastic modulus E (GPa)	209	209	209
Yield strain e_y (%)	0.060	0.130	0.128
Power-law N	0.199	—	—
Bilinear coeff. α	—	0.0025	0.0020

is no plastic work in the deformation of the peel arm, then the plot passes through the origin. However, when the plastic deformation work is large (as is the case for the data in Figure 8), then the line will pass through a negative value on the abscissa. The magnitude of the intercept is the amount of plastic work.

Mandrel data were also obtained with the fully bonded laminates, and these results are presented in combination with the calibration data in Figure 9 (the coefficient of correlation, R^2, for the data for the bonded laminate is generally lower; the value for the data in Figure 9 is 0.997188). Also included on this plot is the result from the fixed-arm test, which can be interpreted as a mandrel peel test with zero alignment force.

The data in Figure 9 enable various calculations to be made, namely adhesive fracture toughness, coefficient of friction, and plastic deformation energy. In this case the adhesive fracture toughness is determ-

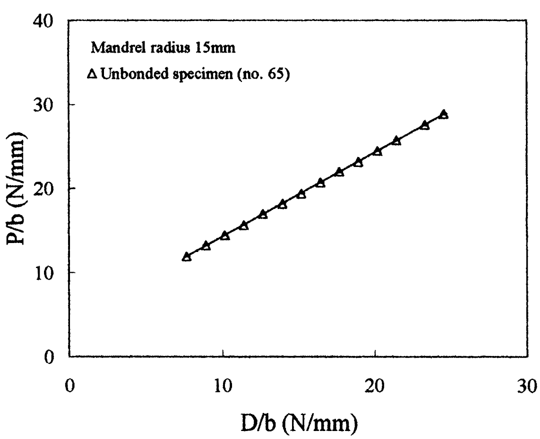

FIGURE 8 Plot of peel force against alignment force (both per unit width) for 1 mm AA with a mandrel of radius 15 mm.

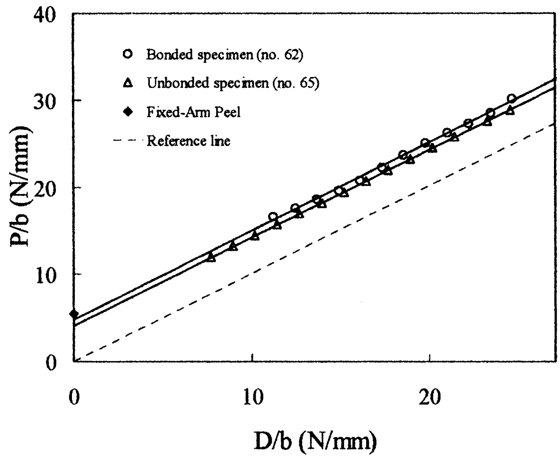

FIGURE 9 Example of peel force against alignment force (both per unit width) diagram. The peel arm is 1 mm AA with rubber-toughened epoxy adhesive. Mandrel radius 15 mm.

ined to be 825 J/m^2, the coefficient of friction is 0.02 (2%), and the plastic work is 4674 J/m^2. This low level of friction in the mandrel tests is typical for all experiments.

The data associated with peel of the bonded specimen generally exhibits some scatter. Consequently, at least three specimens were tested per sample in order to minimise the errors for the measured adhesive fracture toughness.

The mandrel peel results with the thinner peel arms (152 μm copper and 152 μ aluminium) exhibited a different type of characteristic. This is shown in Figure 10 for the results for 152 μm aluminium with the RT epoxy adhesive. The plot for the bonded specimens did not give a straight line fit for the data but instead was dependent on the alignment force.

An alternative way of examining this nonlinear behaviour is to obtain a value for adhesive fracture toughness for each point. The magnitude of force per unit width between each "bonded specimen" point and the calibration curve is obtained, and then G_A is plotted against alignment force per unit area. This procedure is conducted for both sets of data in Figures 9 and 10, and the results are shown in Figures 11 and 12.

In Figure 11 (1 mm AA peel arm) the data are scattered around the value of adhesive fracture toughness from the fixed-arm peel test. In Figure 12 (152 μm aluminium peel arm) the data are dependent on

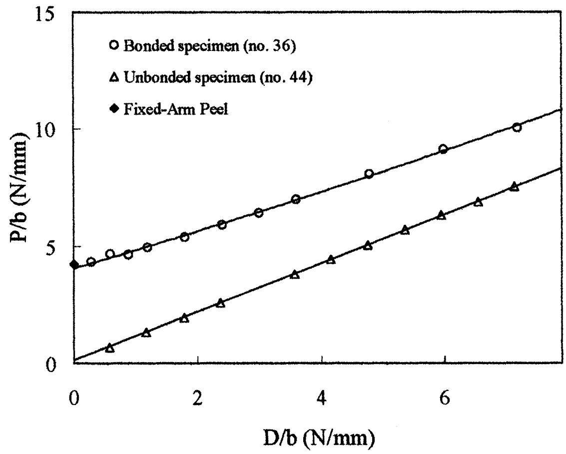

FIGURE 10 Peel force per unit width plotted against alignment force per unit width for 152 μm aluminium/RT epoxy laminate with a mandrel of radius 7.5 mm.

alignment force and converge towards the value of adhesive fracture toughness for the fixed-arm test but never reach this value.

The reasons for this difference in behaviour between laminates with the relatively thin and relatively thick peel arms relates to their ability to conform to the mandrel. Figures 13 and 14 show photographs of

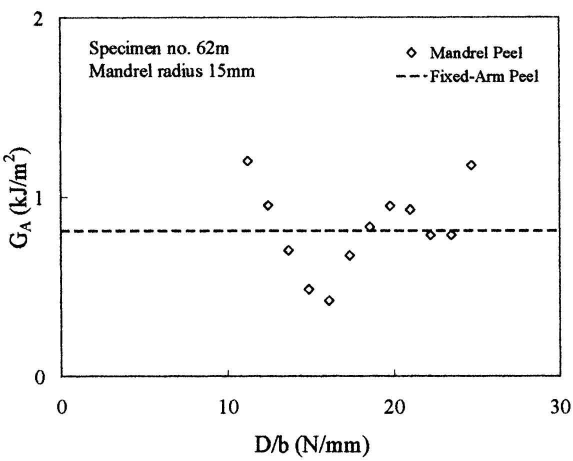

FIGURE 11 Adhesive fracture toughness plotted against alignment force per unit width for 1 mm AA/RT epoxy laminate.

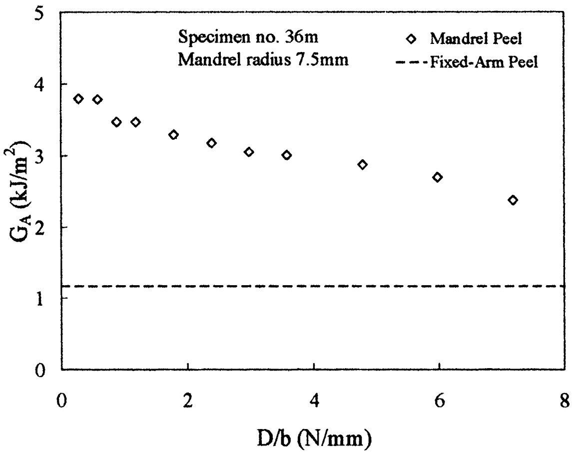

FIGURE 12 Adhesive fracture toughness versus alignment force per unit width for 152 μm aluminium/RT epoxy laminate (NB The value of G_A from the fixed arm test for the 152 micron AA laminate as shown in this figure is higher than that value for the 1 mm AA laminate as shown in Figure 11).

the peel arms during the peel test. The 152 μm aluminium peel arm does not conform to the mandrel while the 1 mm thick AA peel arm does so readily. Even at high alignment loads, the thin aluminium peel arm could not conform to the mandrel and often fractured when higher loads were attempted.

A way of determining whether the peel arm is conforming to the mandrel is by analysing the curves of peel force *versus* alignment force. If bonded and unbonded specimens generate parallel curves over a reasonable range (Figure 9), the peel arm is conformed arround the

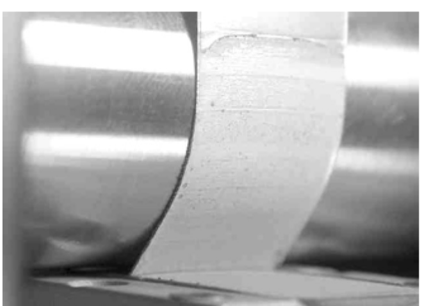

FIGURE 13 Aluminium peel arm 152 μm thickness not conforming to the mandrel of radius 15 mm.

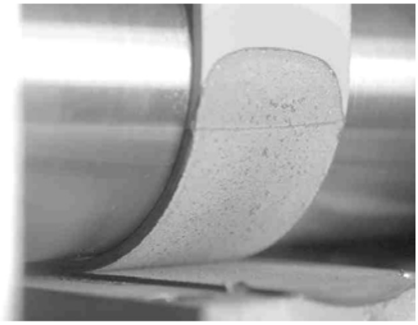

FIGURE 14 AA peel arm 1 mm thickness conforming to mandrel of radius 15 mm.

mandrel and the test is stable (*i.e.*, G_P is constant). If fracture energy is analysed point by point, then a valid test will be characterized by reasonably constant values of G_A, showing no trend when D/b increases but fluctuating around a constant value (Figure 11). That was the case for 1 mm AA and 1 mm steel peel arms.

The results for the thin copper and thin aluminium gave invalid data and were discarded. However, it should be possible to ensure a smooth conformation of the thin peel arms if a smaller radius mandrel were used. It is important to notice that these problems are rare when the adhesive fracture toughness is smaller.

Table 3 gives a summary of results for the valid mandrel peel tests. The results for each peel arm are subdivided according to the size of the mandrel radius. According to the present analysis, the size of the mandrel radius should not influence the measured value for adhesive fracture toughness. Although differences of only 15% have been found between tests with different mandrels, these differences were comparable with the errors involved, so no definitive conclusion could be made in this sense. If we use the overall adhesive fracture toughness values for each peel arm, then it would seem that the value for the 1 mm steel arm is about 30% higher than that for the 1 mm AA peel arm. This would also be the case if data at a common mandrel radius were considered.

The appearance of the peel arm supports this difference in adhesive fracture toughness. The amount of adhesive remaining on the steel arm seems larger than that left on the AA peel arm, although it is currently difficult to quantify this accurately. In both cases it was estimated that an adhesive layer of about 20 μm remained on the peel arm. Primer was not used for the AA peel arms, and this might have accounted for the apparent difference.

TABLE 3 Summary of Mandrel Values for Adhesive Fracture Toughness

			G_A		
Peel arm	Mandrel radius (mm)	Specimen number	Value ± SE* (J/m^2)	Mean ± SD** (J/m^2)	Overall mean ± SD (J/m^2)
1 mm AA	10	68	988 ± 117		
		69	700 ± 73	791 ± 86	
		90	683 ± 144		852 ± 146
	15	62	825 ± 239		
		66	876 ± 52	914 ± 56	
		88	1040 ± 94		
1 mm steel	10	73	1312 ± 146		
		74	1011 ± 277	1114 ± 69	
		75	1019 ± 246		1216 ± 177
	15	82	1459 ± 148		
		83	1198 ± 306	1318 ± 227	
		84	1295 ± 595		

*Standard error.
**Standard deviation.
$SE = SD/\sqrt{n}$, where n is the number of experimental points.

Previous work on the rubber-toughened epoxy adhesive [12] enables the plane-strain plastic zone radius to be calculated from a calculated value for $K_C = 2.05$ MPa $m^{1/2}$ and a measured value for yield stress of 50 MPa, using

$$r_p = \frac{1}{6\pi}\left(\frac{K_c}{\sigma_y}\right)^2. \tag{12}$$

This leads to a value of plastic zone radius of 90 μm. Therefore, despite our coarse measurement of adhesive layer thickness on the peel arm (*Ca.* 20 μm), it is apparent that the development of a plastic zone is being limited during peeling. It is also possible that this limiting mechanism can be different in the 1 mm AA system compared with the 1 mm steel laminate.

Experimental and Theoretical Plastic Work in the Mandrel Peel Test

One of the advantages of the mandrel peel procedure lies in its ability to measure directly the energy associated with adhesive work of fracture and plastic work of deformation during the test. The measurement of plastic work can be compared with the calculated plastic work, as defined in Equations (9) to (11). Figure 15 shows the results of these calculations. It is clear that the agreement between measured plastic work and calculated plastic work is very good.

Fixed-Arm Peel Results

The adhesive fracture toughness can be calculated from a fixed-arm peel test, which determines the peel strength for a peel angle of 90°.

The deformational behaviour of the peel arms were expressed according to the various models described in the above "Tensile Tests" section 3.1. However, two further options were also considered:

1. It could be assumed that the adhesive layer thickness took no part in the bending deformations of the peel arm. This is the option where $h_a = 0$.
2. It could be recognized that the thin layer of adhesive that remained on the peel arm would take part in the bending deformations. Its thickness was estimated to be about 20 μm, *i.e.,* $h_a = 0.02$ mm.

The analysis for conducting these calculations of adhesive fracture toughness for these various options is described in Georgiou *et al.* [7]. Table 4 gives a summary of these various calculations in terms of the values of G_A.

There are varying merits in adopting the options described above. The selection of the tensile stress-strain behaviour depends on the peel arm material. The power law is reasonable for the AA but poor in

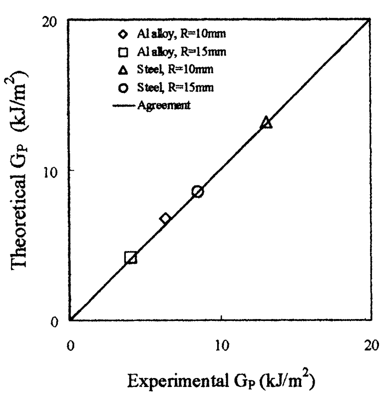

FIGURE 15 Comparison between measured and calculated values of plastic work in mandrel peel tests. Peel arm nominal thickness 1 mm (material parameters from full strain bilinear models).

TABLE 4 Average Values of Adhesive Fracture Toughness (with Standard Deviations) for 1 mm AA and 1 mm steel Rubber-Toughened Epoxy Laminates by Fixed-Arm Peel

	Al alloy $G_A \pm$ SD (J/m^2)		Steel $G_A \pm$ SD (J/m^2)	
Tensile stress-strain model	$h_a = 0$	$h_a = 0.02$ mm	$h_a = 0$	$h_a = 0.02$ mm
Power law function	940 ± 54	986 ± 58	1839 ± 89	2125 ± 107
Full bilinear function	830 ± 62	887 ± 67	1299 ± 78	1619 ± 78
5% strain bilinear function	899 ± 65	952 ± 69	1308 ± 79	1646 ± 93

defining an accurate yield stress for the steel. The full bilinear function is accurate in defining yield and comprehensive in terms of overall deformation for both materials. The 5% strain bilinear function is accurate at defining the yield point but inaccurate for the latter stages of plastic deformation.

A further consideration in the determination of adhesive fracture toughness is the extent of the plastic correction. In using Equation (2) to determine G_A, the plastic correction is given by

$$\text{Plastic correction} = \left(\frac{G_P}{G_E}\right) \times 100\%. \tag{13}$$

Using the data for the full bilinear function with $h_a = 0$, Table 5 summarises the various values for G_A, G_E, and G_P, and includes the values for plastic correction as well.

The plastic corrections are relatively large (86% for the 1 mm AA and 91% for the 1 mm steel). Despite such large corrections, there is good consistency in the results on the six specimens. Although the

TABLE 5 Fixed-Arm Peel Results for Full Bilinear Function with $ha = 0$ Showing Plastic Corrections

1 mm AA					1 mm steel				
Specimen number	G_A (J/m^2)	G_E (J/m^2)	G_P (J/m^2)	Plastic correction (%)	Specimen number	G_A (J/m^2)	G_E (J/m^2)	G_P (J/m^2)	Plastic correction (%)
68	926	6368	5442	85	73	1394	14048	12654	90
69	830	5879	5049	86	74	1351	13771	12420	90
90	849	5971	5122	86	75	1228	12945	11717	91
62	743	5439	4696	86	82	1222	12920	11698	91
66	789	5672	4883	86	83	1360	13823	12463	90
68	845	5960	5115	86	84	1236	13006	11770	91

absolute accuracy of the final adhesive fracture toughness is likely to be influenced by such a large level of correction, it is not believed that this accounts for the difference in fracture toughness between the 1 mm AA and 1 mm steel substrates. The mandrel data for adhesive fracture toughness also confirm this conclusion.

Comparison of G_A from Mandrel Peel and Fixed-Arm Peel

The values of adhesive fracture toughness from the fixed-arm peel tests can be compared with those from the mandrel peel tests. All of the options described in the previous section have been included in

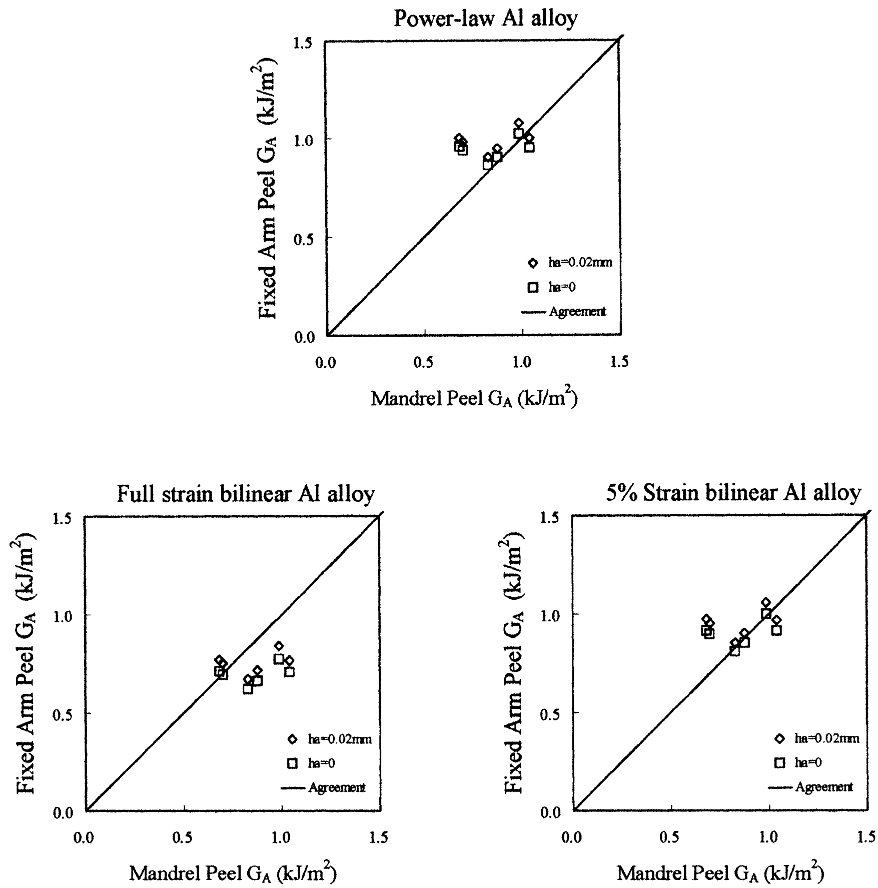

FIGURE 16 Comparison of adhesive fracture toughness from mandrel and fixed-arm peel tests 1 mm AA and rubber-toughened epoxy resin laminates.

this comparative study of adhesive fracture toughness. Figure 16 shows the comparison for the laminates with the 1 mm AA peel arm and Figure 17 shows those for the laminate systems with the 1 mm steel peel arm.

In the case of the comparisons where no consideration is given to the thickness of the adhesive layer, the agreement between adhesive fracture toughness between the two methods (mandrel and fixed-arm peel) is good for either bilinear function in the case of the steel laminates but favours the 5% strain bilinear case for the aluminium laminates. However, when the calculations are conducted for a thin (20 μm) layer of adhesive on the peel arm, the agreement is not as good for any of the definitions of the tensile stress-strain behaviour.

It is assumed that the mandrel peel results give a correct value for adhesive fracture toughness because these are direct experimental measurements. Moreover, the good agreement between plastic deformation energy measured from the mandrel test with the theoretical calculations also suggests that the mandrel procedure is a reliable approach.

In the fixed-arm peel procedure, the analysis for plastic deformation involves the calculation of the root rotation term and the maximum curvature of the peel arm, as discussed in Georgiou *et al.* [7]. These calculations are different depending on whether the thickness of the adhesive layer is included. It is possible that the process of calculating the curvature of the peel arm is where the problem lies, when determining the adhesive fracture toughness from the fixed arm test. On the surface, it would seem that there are fewer problems when the deformations in the adhesive layer are ignored.

CONCLUSIONS

A mandrel peel test has been developed in order to obtain a direct experimental measurement of adhesive fracture toughness for metal/rubber-toughened epoxy laminates. The procedure also provided a measurement for the plastic work dissipated in bending the peel arm around a mandrel. Such direct experimental measurements have an elegant simplicity compared with the vagaries associated with other methods.

Comparisons of adhesive fracture toughness were made with measurements from a 90° fixed-arm test procedure. In order to conduct the calculations in the fixed-arm peel test it was first necessary to model the tensile stress-strain behaviour of the peel arm and second to establish how to deal with possible deformations in the adhesive layer thickness. The tensile stress-strain behaviour of the peel arms

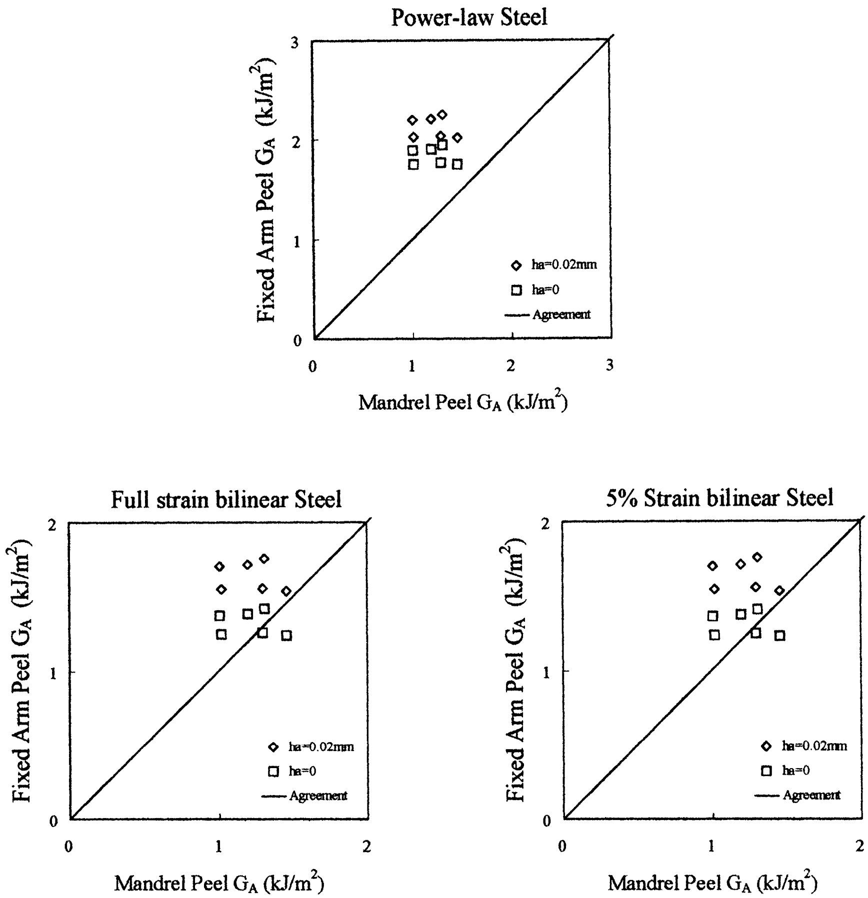

FIGURE 17 Comparison of adhesive fracture toughness from mandrel and fixed-arm peel tests for 1 mm steel and rubber-toughened epoxy resin laminates.

in this work was not easily described by bilinear or power law functions. Moreover, there seem to be some doubts associated with dealing with deformations in the adhesive thickness layer.

On the other hand, the results from the mandrel test appears to be reliable and reproducible. The method seems to be suitable for laminates where the plastic deformation of the peel arm is large. For thin peel arms with high toughness adhesives, tensile yielding of the peel arm often occurs before the peel arm can adequately conform to the mandrel. This difficulty might be avoided if small mandrels are employed.

REFERENCES

[1] *Standard test method for peel resistance of adhesives (T-Peel)*, ASTM D 1876-95 9 (1995).
[2] *Standard test method for climbing drum peel for adhesives*, ASTM D 1781-93 (1993).
[3] *Standard test method for floating roller peel resistance of adhesives*, ASTM D 3167-97 (1997).
[4] *Standard test method for peel or stripping of adhesive bonds*, ASTM D903-98 (1998).
[5] Kinloch, A. J., Lau, C. C., and Williams, J. G., *Int. J. Fract.*, **66**, 45–70 (1994).
[6] Moore, D. R. and Williams, J. G. ESIS 3rd Conference *Fracture of Polymers, Adhesives and Composites*, Blackman, B. R. K., Pavan, A., and Williams, J. G., eds., ESIS pub 32 ISBN 008044195-5, Elsevier (Oxford), p. 341 (2003).
[7] Georgiou, I., Hadavina, H., Ivankovic, A., Kinloch, A. J., Tropsa, V., Williams, J. G., *J. Adhesion*, **79**, 1–27 (2003).
[8] Lau, C. C., PhD Thesis, University of London, London, UK (1995).
[9] Imperial College London Website, *http://www.me.ic.ac.uk/AACgroup/* Peel Test Protocols, IC Peel.
[10] Gent, A. N. and Kaang, S. Y., *J. Adhesion* **24**, 173–181 (1987).
[11] Breslauer, E. and Trocynski, T., *J. Adhesion Sci. Technol.*, **12**(4), 367–382 (1998).
[12] Paraschi, M., A Fracture Mechanics Approach to the Failure of Adhesive Joints, PhD thesis, University of London, London, UK (2001).